Instrumental Development

(2B1)

Construction of Electron-Ion Coincidence Analyzer Using a Polar-Angle-Resolved Compact Time-of-Flight Ion Mass Spectrometer with Three Concentric Anodes

Eiichi KOBAYASHI[*1,*2], Kouji ISARI[*3], Masanobu MORI[*4], Kazuhiko MASE[*1], Koji OKUDAIRA[*4,*5,*6], Kenichiro TANAKA[*3], Nobuo UENO[*4,*6], Shin-ichi NAGAOKA[*7]

[*1]*Institute of Materials Structure Science, 1-1 Oho, Tsukuba 305-0801, Japan*
[*2]*Present address; National Institute of Advanced Industrial Science and Technology, Tsukuba Central 5, 1-1-1 Higashi, Tsukuba 305-8565, Japan*
[*3]*Graduate School of Science, Hiroshima University, 1-3-1 Kagamiyama, Higashi-Hiroshima 739-8526, Japan*
[*4]*Graduate School of Science and Technology, Chiba University, 1-33 Yayoi-cyo, Inage-ku 263-8522, Japan*
[*5]*Institute for Molecular Science, 38 Nishigounaka, Myodaiji-cho, Okazaki 444-8585, Japan*
[*6]*Faculty of Engineering, Chiba University, 1-33 Yayoi-cyo, Inage-ku 263-8522, Japan*
[*7]*Department of Material Science, Ehime University, 2-5 Bunkyo-cyo, Matsuyama 790-8577, Japan*

When a surface is irradiated by X-rays, ions are desorbed by the following three step processes: 1) a core-electron emission (-0.1 fs), 2) an Auger transition leaving two valence holes (1-10 fs), 3) ion desorption due to hole-hole Coulomb repulsion and electron missing from valence orbitals (10-100 fs) (Auger stimulated ion desorption (ASID) mechanism) [1]. For study of the ASID mechanism, coincidence measurements of energy-selected electrons and mass-selected ions (electron-ion coincidence (EICO) spectroscopy) is a powerful technique, because core-excitation-final states or Auger-final-states leading to ion desorption are directly identified [2]. The information on the coincidence ions, however, has been limited to mass and yield, so far. In order to obtain information on kinetic energy and desorption polar angle distributions of ions, we have developed a new EICO apparatus using a coaxially symmetric mirror electron energy analyzer [3] and a compact polar-angle-resolved time-of-flight ion mass spectrometer (TOF-MS) with three concentric anodes.

Figures 1 and 2 show the cross section and photographs of the polar-angle-resolved compact TOF-MS with three concentric anodes, respectively.

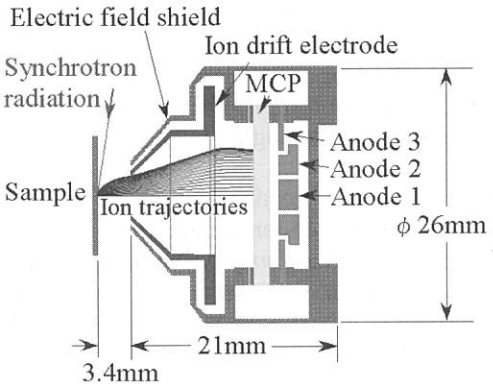

Fig. 1 Cross section of a polar-angle-resolved compact TOF-MS with three anodes. The TOF-MS consists of an electric field shield, an ion drift electrode with three meshes, MCP, and three concentric anodes. Trajectories for ions with a kinetic energy of 2 eV from a pointed source are shown for the desorption polar angles of 0°～90° with 5° step based on the simulation with SIMION 3D version 7.0. The voltages of the sample, the drift electrode and the entrance of the MCP are 0, -30 and -2000 V, respectively.

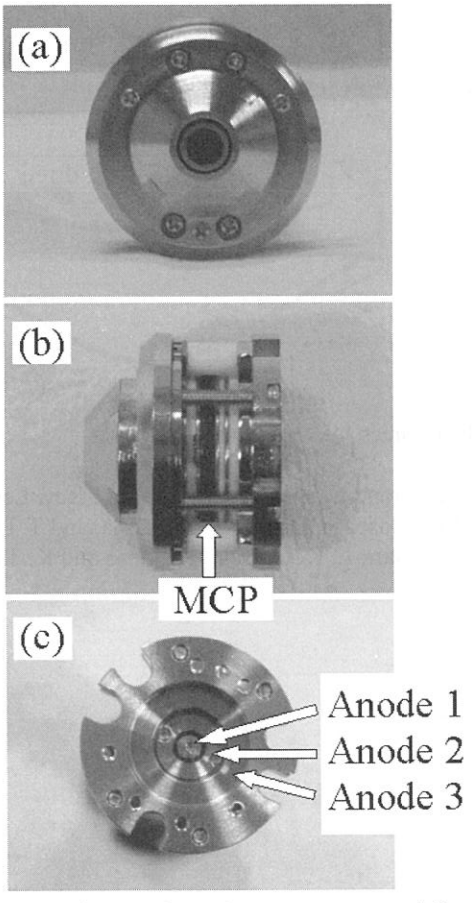

Fig. 2 Photographs of the polar-angle-resolved compact TOF-MS with three concentric anodes. (a) The front view, (b) the side view, and (c) the three concentric anodes.

The polar-angle-resolved TOF-MS is composed of a drift electrode, an electric field shield, and MCP with three concentric anodes. The MCP was constructed from

commercial one (Hamamatsu photonics, F4655). The outer diameter of the innermost anode (anode 1) is 3.0 mm, and the inner and outer diameters of the middle anode (anode 2) and the outer anode (anode 3) are 4.0, 8.0, 9.0, and 14.5 mm, respectively. Figure 3 shows a contour line chart where the characteristics of this TOF-MS are described, that is, ion desorption polar angle and kinetic energy dependency of the time-of-flight (TOF) and the detected anode. When the TOF of a coincidence ion is measured by the individual anodes as a function of the drift bias, the desorption polar angle and the kinetic energy of the ion are estimated from the Fig. 3.

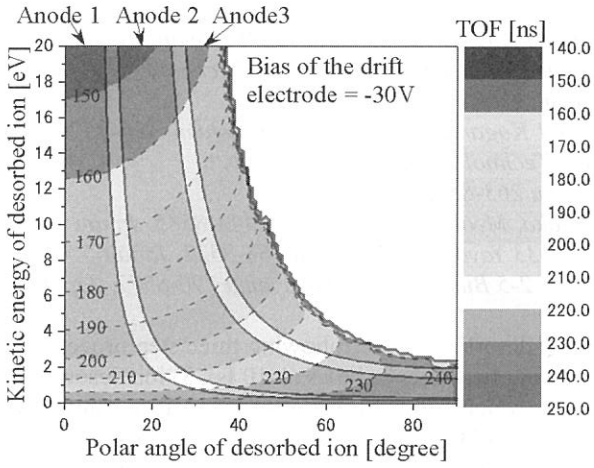

Fig. 3 Contour map of TOF of H^+ for the compact TOF-MS with three anodes as a function of the desorption polar angle and the kinetic energy. The geometry and the electrode voltages are the same to those of **Fig. 1.**

A new EICO apparatus using a coaxially symmetric mirror electron energy analyzer [3] and the polar-angle-resolved compact TOF-MS is shown in Fig. 4. Features of the electron – polar-angle-resolved ion coincidence analyzer are as follow: 1) The desorption polar angle and kinetic energy distribution of the coincidence ions can be estimated for the selected core excitations or the Auger-final-states. 2) The atoms or molecules responsible for the ion desorption can be identified from the desorption polar angle and the mass. For instance, in the case of fluorinated Si(111), F^+ desorbed in the surface normal direction can be assigned to the –SiF, while F^+ desorbed in the surface off-normal direction can be assigned to the $–SiF_3$. 3) One can clarify how the ion desorption mechanism is different according to the desorption polar angle

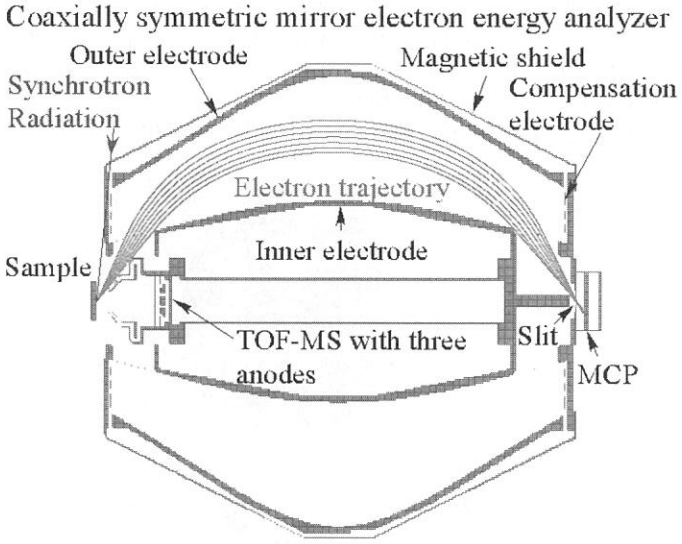

Fig. 4 Cross section of a electron – polar-angle-resolved-ion coincidence analyzer which consists of a coaxially symmetric mirror electron energy analyzer [3] and the polar-angle-resolved compact TOF-MS with three anodes.

References

[1] R. Franchy and D. Menzel, Phys. Rev. Lett. 43 (1979) 865.
[2] K. Mase, S. Tanaka, S. Nagaoka, and T. Urisu, Surf. Sci. 451 (2000) 143.
[3] K. Isari, E. Kobayashi, K. Mase and K. Tanaka, Surf. Sci., 528 (2003), 261.

(BL5B)

Quantum Efficiency Measurements of a Back-illuminated CCD for Solar-B X-Ray Telescope

[A] H. Hara, [A] R. Kano, [A] K. Kumagai, [B] T. Sakao, and [A] S. Tsuneta

[A] *National Astronomical Observatory, Mitaka, Tokyo 181-8588*
[B] *Institute of Space and Astronautical Science, Sagamihara, Kanagawa 229-8510*

Solar-B X-ray telescope (XRT) is being developed in collaboration with US group and Japanese group is developing an X-ray camera as its detector and an on-board computer for the automatic control of telescope operation. XRT is a 3 m-long gazing-incidence telescope and has a spatial resolution of 2 arcsec. It covers a wide spectral range from soft X-ray to EUV range owing to adoption of a back-illuminated CCD. We are expecting high-resolution images for the study of the solar corona after the launch of Solar-B, which is a spacecraft of Institute of Space and Astronautical Science (ISAS), and will challenge to solve a question why the solar corona is formed in conjunction with the Solar Optical Telescope and EUV Imaging Spectrometer aboard Solar-B.

We have developed a CCD camera with a back-illuminated CCD for an EUV observation of the solar corona and launched an EUV telescope with the ISAS S520CN-22 sounding rocket in 1998 [1]. The calibration of the CCD camera, filters, and EUV multilayer mirrors was performed at BL5B [2), 3)]. Since the pass band of the EUV telescope was so narrow that the quantum efficiency of CCD can be considered as a flat spectral response, the quantum efficiency (QE) of the EUV camera was simply estimated by comparing the current of a calibrated EUV photo diode and CCD outputs. On the other hand, XRT has a broad spectral response from soft X-ray (0.2 nm) to EUV range (40 nm), resulting in more complicated process in QE measurements. Since the mission duration of a satellite program is more than three years, much longer than 5 min observing time in the sounding rocket program, the contamination to the flight-model camera during the QE measurement has to be stringently controlled.

After a test of long-duration soft X-ray and EUV irradiation to a back-illuminated CCD [4], which was performed at BL5B for a selection of Solar-B XRT CCD from a point of view of the on-orbit radiation hardness, we built a test facility for QE measurement of an X-ray CCD camera in our laboratory at National Astronomical Observatory of Japan (NAOJ). Since it did not have capability of CCD calibration in EUV range at the initial phase, we planned to use the UVSOR synchrotron beam for the QE measurement and did several measurements in 2002. Although we were originally going to make the QE measurement of the flight-model (FM) CCD at UVSOR, we could not execute it due to several reasons. One major reason is a delay of completion of FM camera electronics, and the other major reason is that we felt that we cannot easily control the cleanliness level in the BL5B chamber. We measured the outgas in BL5B calibration chamber with a contamination monitor, the so-called TQCM, and found that the rate of deposition of contaminants on the TQCM crystal whose temperature is –15 degree C is about 100 Hz/hour, which

corresponds to a deposition thickness of 1.0 nm/hour. In the reflectance measurement of multilayer mirrors we have not experienced the reduction of reflectance during the measurement. We think that contaminants could not be deposited to the multilayer mirrors owing to a high-temperature (about 40 deg C) condition of mirrors during the measurements and that a cooled CCD condition is quite different from the contamination-control point of view.

We did three measurements at UVSOR for calibration of XRT CCD camera in 2002: 1. filter-transmittance measurement of a proportional counter for absolute calibration (Fig.1), 2. cross calibrations of several SSD used as a reference detector, 3. quantum efficiency measurement of proto-model (PM) CCD (Fig.2). After the UVSOR measurements in 2002 we set an EUV monochrometer at NAOJ for calibration in EUV range and we have a capability to calibrate CCD from soft X-ray to EUV range at present as shown in Fig.2. FM CCD is going to be calibrated at NAOJ.

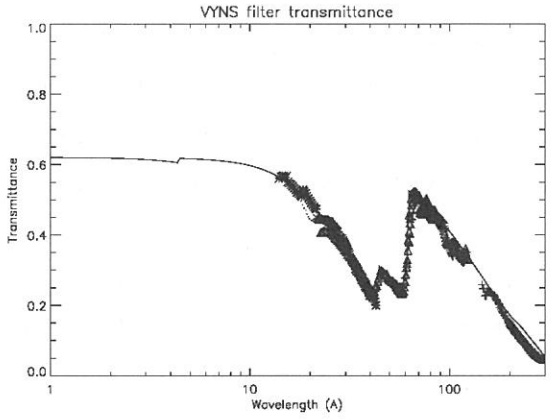

Fig. 1: Filter transmittance of a proportional counter for absolute calibration. Solid line indicates a model estimated from the elemental compositions of filter materials.

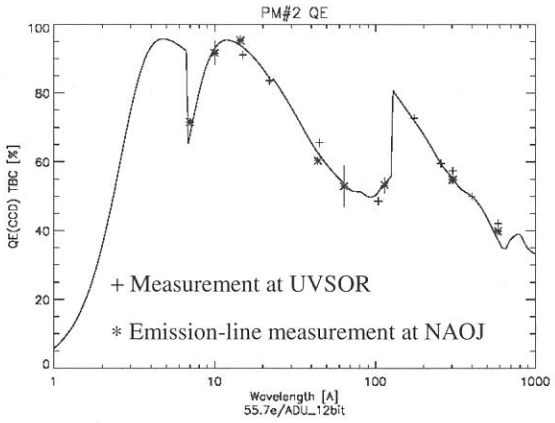

Fig.2: Quantum efficiency of Solar-B XRT proto-model CCD. Solid line indicates a back-illuminated CCD model.

References

1) T. Sakao et al., *Solar Phys.*, **187**, 303, (1999).
2) S. Nagata et al., *Applied Opt.*, **36**, 2830, (1997).
3) H. Hara et al., *Applied Opt.*, **38**, 6617, (1999).
4) R. Kano et al., *Report of the National Astronomical Observatory of Japan*, **6**, 19, (2000).

(BL5B)

Calibration of Mo/Si multilayer-coated gratings

[A] Shingo Kameda, [A] Hideo Sagawa, [A] Tetsunori Murachi, [A] Miho Kanao
[B] Atsushi Yamazaki, and [A] Ichiro Yoshikawa

[A] *Institute of Space and Astronautical Science, Sagamihara, Kanagawa 229-8510*
[B] *Communications Research Laboratory, Koganei, Tokyo 184-8795*

An extreme ultraviolet imaging spectrometer (EUIS) for the Mercury mission is under development. The instrument is designed to measure extreme ultraviolet radiations from the atmosphere of Mercury, which could not be identified by the Mariner 10 mission [1]. In this report, the performance of a Mo/Si multilayer grating, which is newly developed optics to improve the diffraction efficiency in the EUV, is presented. Two types of grating are fabricated, i.e. mechanical ruling and holographic gratings.

In this experiment, we used a blazed mechanical ruling plane grating (blaze angle 8.38° , blaze wavelength 250nm) and a blazed holographic plane grating (blaze angle 7.9° , blaze wavelength 229nm). To improve the diffraction efficiency at 30.4nm, we coated these gratings with 10 pairs of Mo (5nm) and Si (15nm) layer.

Figure 1 shows the diffraction image of each grating. In the mechanical ruling grating (Fig. 1(a)), the diffraction light is relatively difficult to find due to the high intensity of stray light. It is caused by surface roughness of the grating. On the other hand, the diffraction light of the holographic grating is clearly identified as shown in Fig 1(b).

Figure 2 shows the intensity of diffraction light of each grating. The intensity (vertical axis) is normalized with electron beam current. Signal(diffraction light)-to-Noise(stray light) ratio is shown in Table. The result shows that stray light of the holographic grating is 8 times less than that of the mechanical ruling grating.

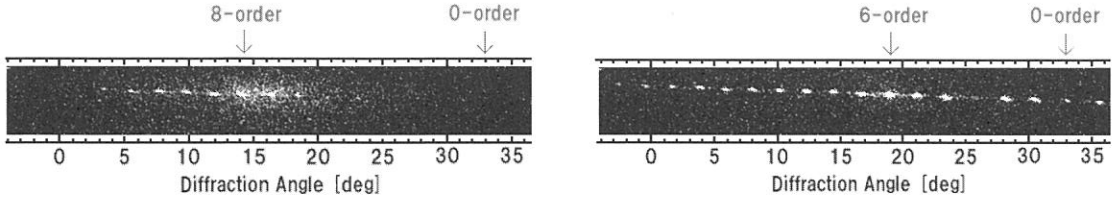

(a) (b)

Fig. 1 Diffraction image of (a) the mechanical ruling grating and (b) the holographic grating
Wavelength : 30.4nm Incident Angle : 33°

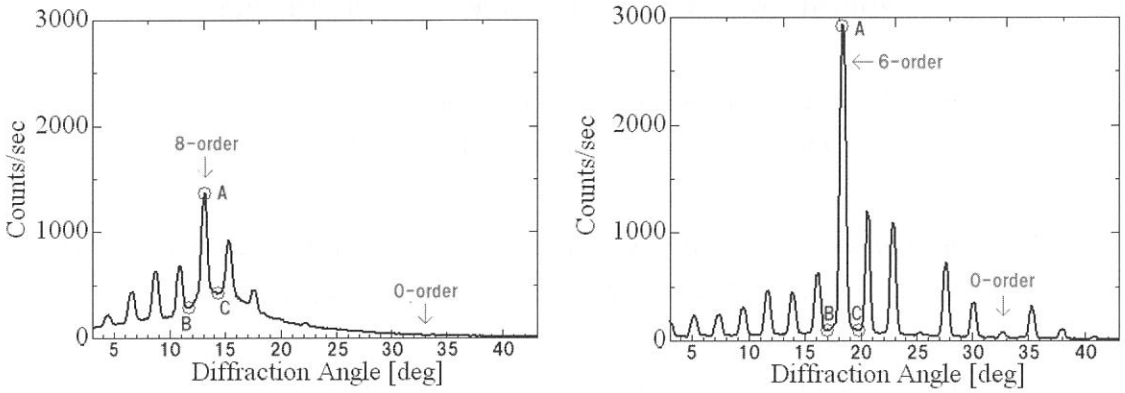

Fig.2 Diffractive distribution of (a) the mechanical ruling grating and (b) the holographic grating

Wavelength : 30.4nm　Incident Angle : 33°

Table Diffraction-stray light ratio (A, B, and C are in Fig.2)

Type of grating	(A)	((B+C)/2)	Ratio [(A):((B+C)/2)]
Mechanical ruling	1330[cts]	343[cts]	26%
Holographic	2935[cts]	93[cts]	3.2%

Reference

[1] Yoshikawa, I., A. Yamazaki, T. Murachi, S. Kameda, H. Sagawa, S. Okano, T. Okada, and M. Nakamura, Development of an Extreme Ultraviolet Imaging Spectrometer for the BepiColombo Mission, *Advances in Space Research,* in press.

(BL5B)

Reflectivity Mesurements of Mo/Si Multilayer Coated on Schwarzschild mirrors

Y. Kondo, J. Azuma* and M. Kamada*

Venture Business Laboratory, Saga University, Honjo, Saga 840-8502, Japan

**Synchrotron Light Application Center, Saga University, Honjo, Saga 840-8502, Japan*

Photoelectron spectroscopy (PES) is one of the most powerful tools to investigate the electronic states dominating property of material. Since with the progress of process technology, semiconductor devices with the size of sub-μm have been made and it is very important to analyze the influences caused by the reaction at interface and impurity on the performance of the devices in sub-μm, microscopic photoelectron spectroscopy (μ-PES) with spatial resolution of sub-μm is strongly demanded. However, the spatial resolution of the conventional PES is limited to about 10 μm because laboratory light source, such as discharge lamp and X-ray tube, have low photon flux density. Therefore, we are presently developing a μ-PES equipment with Schwarzschild objective. This system has high detection efficiency to overcome the disadvantages of laboratory light sources, since it consists of the higher harmonic (λ=17.8 nm) produced by pulsed laser [1], the time-of-flight (TOF) photoelectron analyzer, and Schwarzschild demagnification objective.

Reflection multilayer, which consists of two materials, is necessary to be coated on the Schwarzschild mirrors to obtain the high reflectivity at the wavelength of the higher harmonic (λ=17.8 nm). Two materials (Mo and Si) were selected according to the selection rule of material pairs. The thickness of materials was designed so as to obtain high reflectivity by using layer by layer method. The designed thickness of each layer and the number of layers are Mo (2.8 nm) / Si (6.6 nm) and, 41 respectively. The ranges of the incident angle are from 2.9° to 5.2° for the concave mirror and from 8.0° to 14.2° for the convex mirror as a function of radial direction of Schwarzschild mirrors, respectively. Ideally, the period length of the multilayer should be controlled in the radial direction of Schwarzschild mirrors so as to reflect the light of the same wavelength for every angle of incidence. However, it is not easy to control the thickness of multilayer in such a way. Therefore, the present mirrors were coated with the multilayer within the deviation of the period length of 2 % (d = 9.4 ± 0.2 nm). As a result of the simulation in consideration of the deviation, the reduction of the reflectivity was found to be 20 % at the maximum.

The multilayer were fabricated by magnetron sputtering system (ANELVA SPL-500). The convex (diameter 10 mm) and concave (diameter 40 mm) mirrors were polished at machine shop of Tohoku University for Schwarzschild mirrors. Two mirrors and a Si-wafer for the monitor of the period length were coated with Mo/Si multilayer at the same time. Mo was dc-sputtered by the power of 100 W, and Si was rf-sputterd by the power of 200 W. The Ar pressure was 2.0 mTorr during the deposition and the base pressure was 5.0×10^{-7} Torr. The deposition rates of Mo and Si were 1.65 nm/min. and 1.71 nm/min., respectively. The distribution of the period length of fabricated multilayer in radial direction were evaluated to be 9.3 ± 0.1 nm from analyses of the bragg peaks of X-ray diffraction.

To estimate the throughput efficiency of Schwarzschild objective, the reflectivity of the Mo/Si multilayer coated on Si-wafer was measured at beamline BL5B of UVSOR. The grating and mirror combination of G2 and M3 was used in this experiment and Si filter was inserted to remove the higher order light between the re-focusing mirror and sample. The calibration of wavelength was performed by observing *L*-edge of Al filter. The s-reflectivity spectra of Mo/Si multilayer at the incident angle of 10 deg. are shown in Fig. 1. The dotted line and the solid line are measured and calculated reflectivity spectra of Mo/Si multilayer, respectively. In this figure the measured reflectivity was 38 % around the wavelength of 17.8 nm. On the other hand, the calculated one was 55 % at same wavelength. This reduction of the reflectivity is caused by the roughness and diffusion at the interfaces between Mo and Si, because it can be explained by simulation of the reflectivity in consideration of the roughness and diffusion. The distribution of the reflectivity of Mo/Si multilayer as a function of the distance from center of the multilayer is shown in Fig. 2. With the deviation of the position from the center, the reflectivity decreases a little. This reduction of the reflectivity at the position of $r > 10$ mm is due to be shorter for the period length than the one at the center position ($r = 0$ mm). The reduction of the reflectivity was able to be restricted within 10 % at the maximum by controlling the period length of the multilayer in radial direction. In conclusion, the throughput efficiency of Schwarzschild objective is expected to be >14% and this fabricated system is available as Schwarzschild objective for μ-PES using the higher harmonic (λ=17.8 nm).

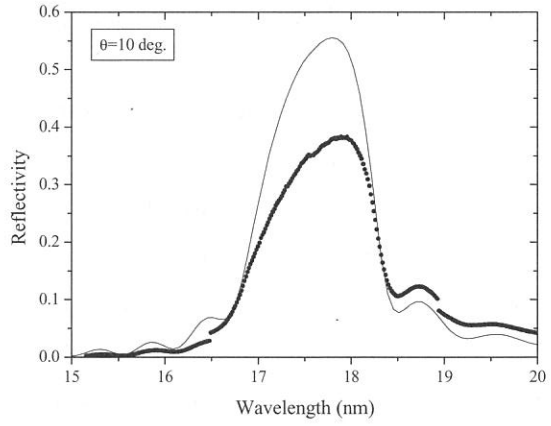

Fig.1 The s-reflectivity spectra of Mo/Si multilayer at incident angle of 10 deg. The dotted line and the solid line present measured data and calculation one, respectively.

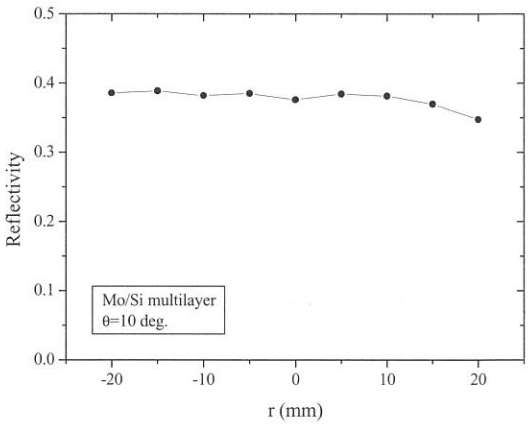

Fig. 2 The distribution of reflectivity in radial direction at the wavelength of 17.8 nm.

Referlence

[1] Richard Haight, Applied Optics Vol.35 (1996) 6445.

(BL5B)

Evaluation of Diffraction Efficiency of a Reflection Grating and Higher Order Contamination of the PGM at BL5B

Akira MIYAKE, Fumitaro MASAKI and Yuzuru TAWARA

Department of Physics, Nagoya University, Chikusa, Nagoya, 464-8602, Japan

Diffraction efficiency of a mechanically-ruled flat field grating[1] (sample grating) was evaluated using BL-5B plane grating monochromator (PGM) with s-polarization condition. G3M3 was used for a wavelength range from 10nm to 21nm and G2M1 was used for a wavelength range from 5nm to 11nm. Foils of boron (t=0.13μm), beryllium (t=0.2μm), silicon (t=0.57μm) and aluminum (t=0.15μm) were used as higher order elimination filters. The sample grating is mounted on a rotational stage at the center of a goniometer and a back illuminated CCD is mounted on a rotating arm of the goniometer. Both angular dependency of the light intensity diffracted by the sample grating and incident beam intensity were measured with the same CCD. In order to intercept the beam on the CCD during charge transfer, a rotating shutter was equipped.

Figure 1 shows an experimental result of angular distribution of diffracted beam intensity at a wavelength of 16.0nm(G3M3) without any filter. The grating constant of the sample grating is 1200 lines/mm. Measurement was performed at a fixed incident angle of 87 degrees. Each observed peak corresponds to a combination of diffraction order of PGM(n) and diffraction order of the sample grating(m). The absolute diffraction efficiency of the sample grating was calculated by normalizing the observed angular dependency of the diffracted light intensity by the incident beam intensity. Figure 2 shows absolute diffraction efficiency of each order.

The higher order contamination of the PGM was estimated using the angular dependency of the diffracted light, measured diffraction efficiency of the sample grating and measured sensitivity of the CCD. Figure 3 shows the intensity ratio of the 2nd order to the 1st order of the PGM. It is confirmed that the 2nd order ratio to the 1st order can be reduced to less than 2% with an adequate filter.

Reference

1. T. Kita, T. Harada, N. Nakano and H. Kuroda, Appl. Opt. **22**, pp.512, 1983.

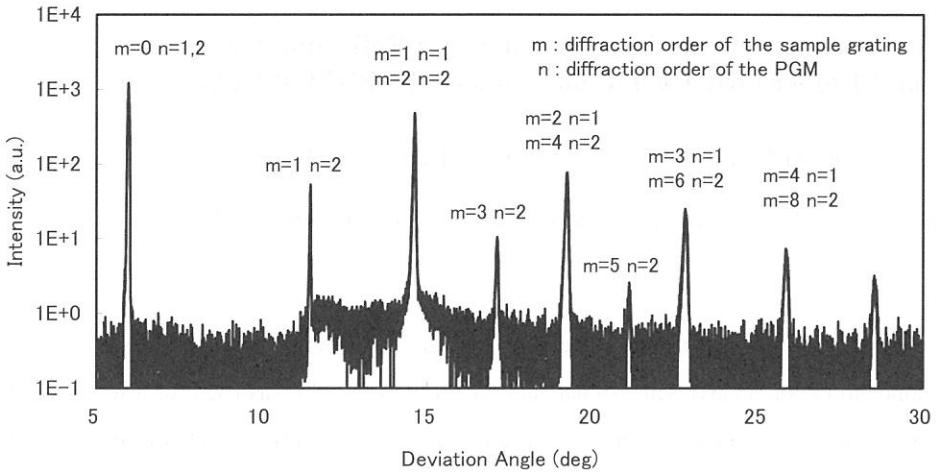

Figure 1. Observed angular distribution of diffracted light

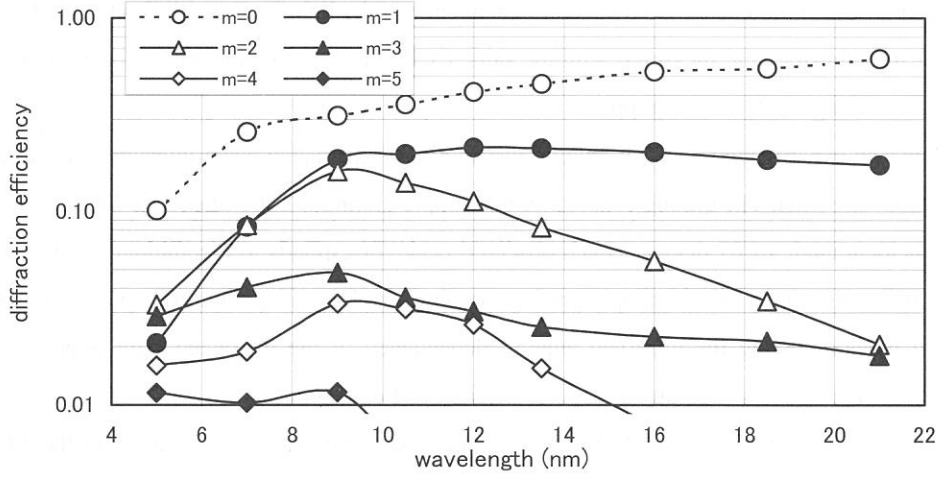

Figure 2. Measured absolute diffraction efficiency of the sample grating

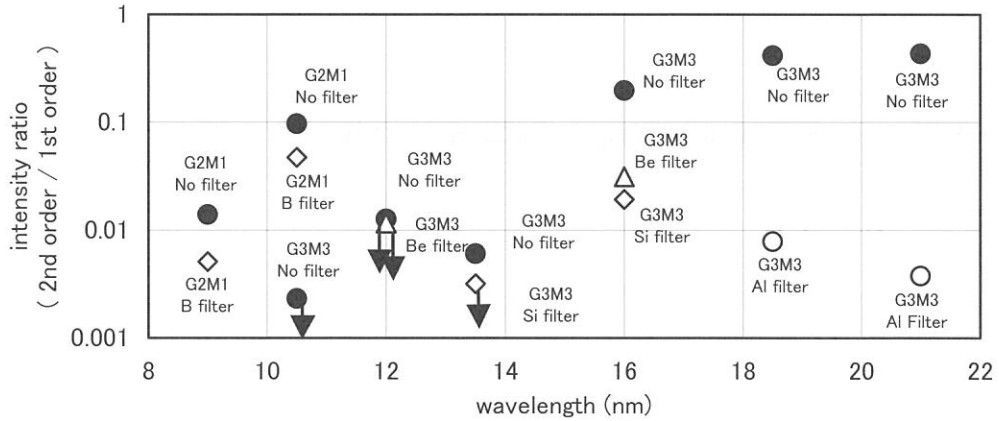

Figure 3. Measured higher order contamination of the PGM

(BL5B)

Fabrication of Mo/Si and Cr/C multilayer polarizers and polarization property measurement of SR in BL5B beam-line

Masahito Niibe and Mikihito Mukai
Himeji Inst. of Technology, Lab. of Advanced Science and Technology for Industry
Kouto 3-1-2, Kamigoori, Ako-gun, Hyogo 678-1205

Soft X-ray multilayer mirrors can be utilized as polarizers, since they have pseudo-Brewster angles in the vicinity of 45deg. incidence angle, and since large difference in reflectivity occurs between s-polarized and p-polarized lights. In this study, polarizers for wavelengths near 13.5 nm and 7 nm were fabricated using Mo/Si and Cr/C multilayers, respectively. The polarization property of SR in the BL5B beam-line was measured using them. It is known that the error is produced for the reflectivity measurement of multilayers near the 45deg. incidence angle by the polarization of light source. By calculating the reflectivity considering the degree of polarization of the light source, the error was able to be reduced.

Mo/Si multilayer (period: 10.5 nm, Si film thickness ratio: 0.6, 30 layer pairs) and Cr/C multilayer (period: 5.43 nm, C film thickness ratio: 0.7, 50 layer pairs) were prepared as polarizers for the wavelengths near 13.5 nm and 7 nm, respectively, using a magnetron sputtering technique. The reflectivity and polarizance of produced multilayers were evaluated using BL5B reflectometer.

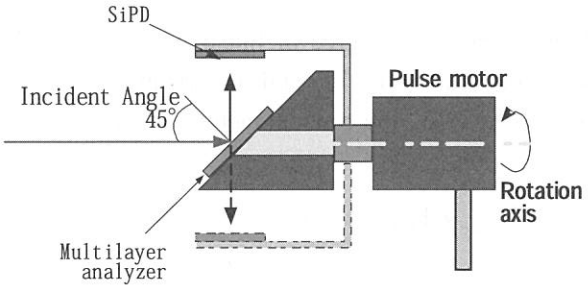

Fig. 1 Rotating analyzer detector

The polarimetry was carried out by Rotating-Analyzer Ellipsometry (RAE) method[1]. The schema of rotating analyzer detector produced in this study is shown in Fig. 1. It is rather small type; the overall length is about 200 mm. A stepping motor was used in the rotating analyzer, and the angular resolution of azimuth was 0.024 deg.

The polarizance measurement of the multilayers was carried out by the polarimetry of the soft X-rays reflected by the multilayer mirror as a polarizer at 45 deg. incidence. The measurement wavelengths were 13.8 nm for Mo/Si multilayer and 7.48 nm for Cr/C multilayer. The measurement result for Mo/Si multilayer is shown in Fig. 2 and that for Cr/C multilayer is shown Fig. 3. The solid circles in each figure denote measured values, and the continuous lines denote cosine square fitting by Malus' law. The reflected

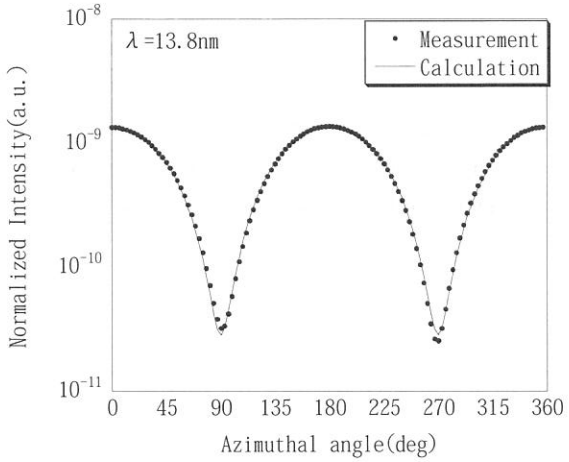

Fig. 2 Polarizance measurement of Mo/Si multilayer.

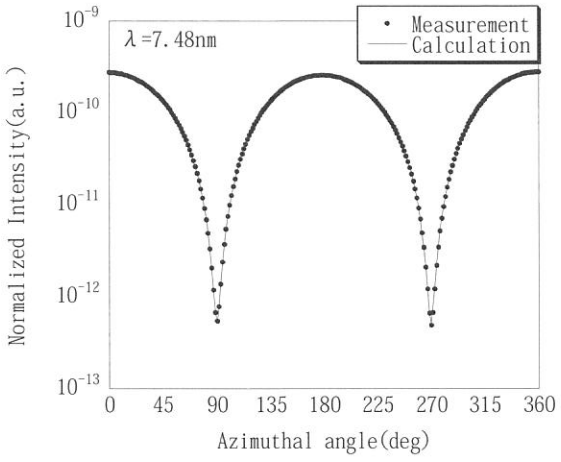

Fig. 3 Polarizance measurement of Cr/C multilayer.

light from the polarizer seems to be almost linearly polarized light. Then, polarizance of the analyzer was calculated to be 0.959 for the Mo/Si multilayer and 0.996 for the Cr/C multilayer.

On the basis of the polarizances of multilayer analyzers, degree of linear polarization of SR in the BL5B beam-line was measured. The measurement was carried out by the RAE method with directly introducing the SR right to the analyzer. The Mo/Si multilayer was used as the analyzer at the 13.8nm wavelength. The measurement result is shown in Fig. 4. The solid circles in the figure denote measured values, and the continuous line is the cosine square fitting.

The contrast factor, C_{ont}, of the observed intensity is written by following equation with the maximum intensity, Imax, and minimum intensity, Imin, of incident light on the analyzer detector.

$$C_{ont} = \frac{\mathrm{Imax} - \mathrm{Imin}}{\mathrm{Imax} + \mathrm{Imin}} \qquad (1)$$

If we denote the degree of linear polarization of the light source by P_L and polarizance of the analyzer by P_{zance}, the contrast factor is obtained as

$$C_{ont} = P_{zance} \times P_L . \qquad (2)$$

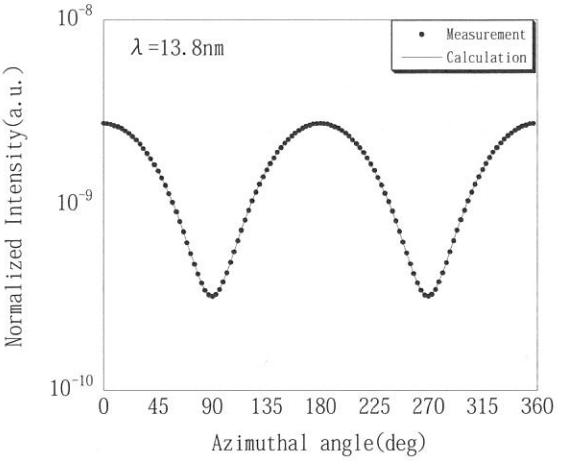

Fig. 4 Measurement of the degree of linear polarization of the SR light in BL5B beam-line at λ=13.8nm.

From equation (1) and (2), the degree of linear polarization of lights in the BL5B beam-line was obtained and which value was 0.821.

The reflectivity of multilayers at 45 deg. incidence angle were calculated considering the degree of linear polarization of the light source. The result of Cr/C multilayer is shown in Fig. 5. From the figure, it is proven that calculated value in Cr/C multilayer agrees well with the measured value.

1) Kimura et al., SPIE vol. **2010** 37-44 (1993).

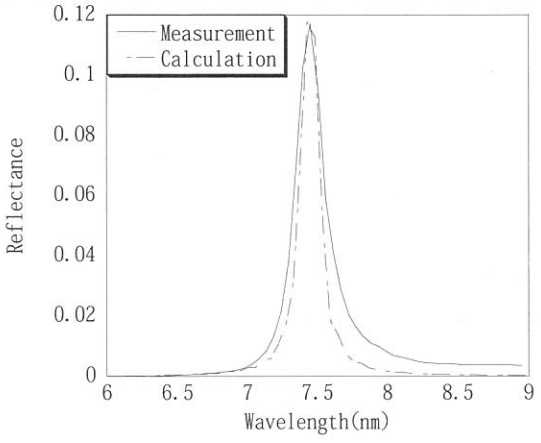

Fig. 5 Reflectivity of Cr/C multilayer at 45 deg. incidence angle calculated with concerning the degree of linear polarization of light source.

High-energy-resolution angle-resolved photoemission spectroscopy apparatus at BL5U

S. Kimura, K. Takahashi*, T. Ito, K. Soda[1], T. Takeuchi[2], K. Shinba[1], T. Kondo[1], T. Nakagawa[3] and N. Kosugi

UVSOR Facility, Institute for Molecular Science, Okazaki 444-8585
[1]Department of Crystalline Materials Science, Nagoya University, Nagoya 464-8603
[2]Research Center for Advanced Waste and Emission Management, Nagoya University, Nagoya 464-8603
[3]Department of Molecular Structure, Institute for Molecular Science, Okazaki 444-8585

We have constructed a new high-energy-resolution angle-resolved photoemission apparatus shown in Figure 1 for the helical undulator beam line, BL5U. The main purpose is the investigation of the electronic structure near the Fermi level as well as the topological shape of the Fermi surface, so-called "Fermiology", of solids, thin films and surfaces. The apparatus consists of a photoelectron analyzer, a main chamber, a sample preparation chamber, a liquid-He flow-type cryostat (JANIS ST-400 UHV) with a manipulator, a He lamp with UV monochromator (GAMMADATA VUV5000 + VUV5040) and several vacuum pumps. Samples are transferred to the preparation chamber from a load-lock chamber, a molecular beam epitaxy system or other chambers that can be replaced by users.

The main part of the apparatus is a new type hemispherical photoelectron analyzer with 200-mm main radius, MBS-Toyama A-1, we call it "Peter analyzer". The energy resolution is better than previous one, *i.e.*, the line width of Xe $5p_{3/2}$ photoemission is about 3.12 meV at 1-eV pass energy (Figure 2). Since the line width includes the doppler shift of the Xe gas and the width of the He lamp, the energy resolution of Peter analyzer is evaluated to be less than 1 meV. The same resolution was obtained by the measurement of the Fermi edge of Au at low temperatures (Figure 3). Six pass energies from 1 to 50 eV can be selected. The resolving power (E / ΔE) is about 1,800 in all pass energy. The angler resolution is less than 0.5 degree.

The main experiment of the apparatus is to measure angle-resolved photoemission spectra. The test using a He lamp is in progress.

The apparatus that will be installed at BL5U in September 2003 is used for angle-resolved

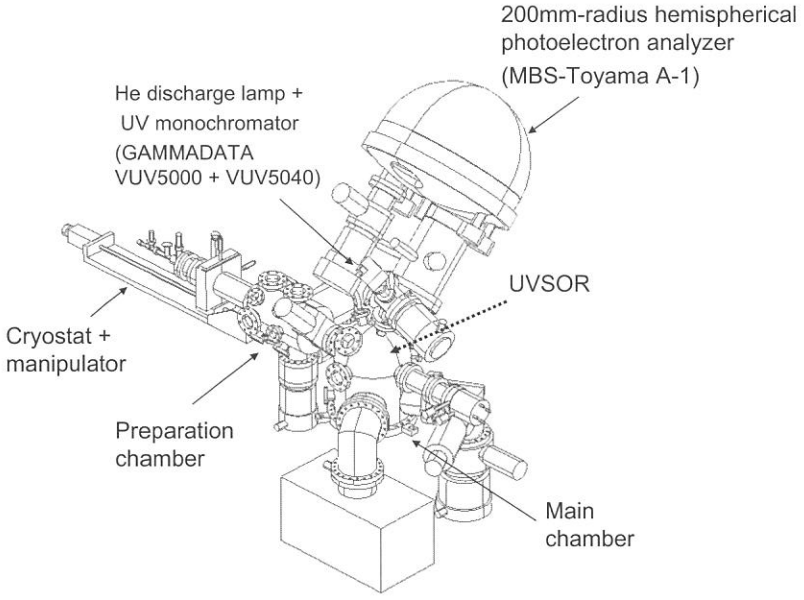

Fig. 1. High-energy-resolution angle-resolved photoemission apparatus for BL5U.

photoemission measurements with tunable photons of the energy and the polarization (linear / circular) from the helical undulator at BL5U [1].

References

* Present address: Synchrotron Light Application Center, Saga University, Saga 840-8502

[1] S. Kimura *et al.*, J. Synchrotron Rad. **5**, 453 (1998).

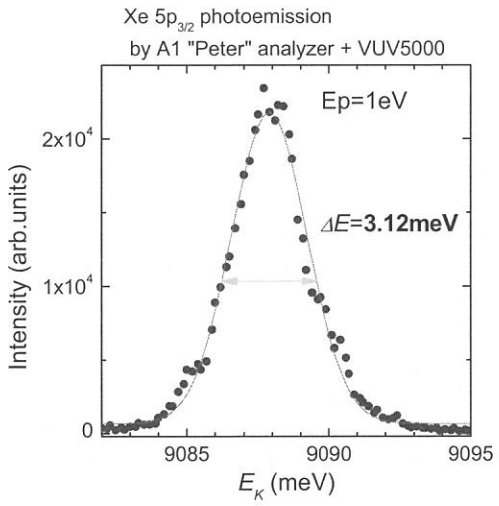

Fig. 2. Xe $5p_{3/2}$ photoemission peak for the resolution test of A-1 analyzer. The peak width (ΔE = 3.12 meV) includes the Doppler shift of Xe gas (~ 3 meV) and the line width of the He lamp (~ 0.9 meV).

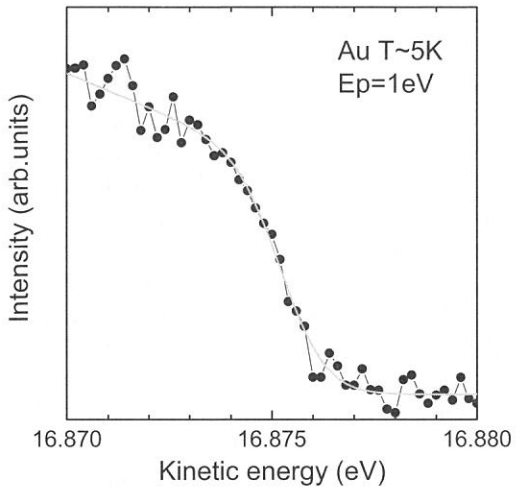

Fig. 3. Fermi edge spectrum of Au at around 5 K with 1 eV pass energy. The energy resolution of the analyzer is evaluated to be less than 1 meV.

(BL6A1)

Spectromicroscopy in the terahertz region at BL6A1

S. Kimura[1,2] and T. Nishi[2]

[1]*UVSOR Facility, Institute for Molecular Science, Okazaki 444-8585*
[1]*Department of Structural Molecular Science, The Graduate University for Advanced Science, Okazaki 444-8585*

Infrared synchrotron radiation (IR-SR) is very powerful for an IR spectromicroscopy with the spatial resolution of the diffraction limit because of its low emittance nature. Therefore more than fifteen IR-SR beam lines, which are mainly used for the IR-SR spectromicroscopy in the region of the mid-IR – the near-IR, have been constructed up to now in the world [1]. On the other hand, since the photon flux of SR in the terahertz as well as the far-IR region is several orders higher than that of ordinary light source in the region, for instance a mercury lamp, the spectromicroscopy using SR in the region has the advantage for the ordinary light source. In addition, since many rotational modes of protons, vibrational modes of heavy molecules and carrier absorption of quasiparticles of strongly correlated systems appear in the terahertz region, the development of the spectromicroscopy method is very important in the future. Then we tested the terahertz spectromicroscopy using SR is useful or not.

The experiment was done at the IR beam line, BL6A1. An IR microscope made by BUNKO-KEIKI Co. Ltd. was installed at the free port of the beam line. SR was led to a FTIR spectrometer Bruker IFS66v and to the IR microscope. Figure 1 is the obtained throughput spectra using UVSOR and globar lamp mounted in the FTIR. Since the photon flux from UVSOR is two orders higher than that from the globar lamp, the difference appears in the figure. Top of the figure 2 is the intensity plot of a gold mirror edge vs position and the bottom the first derivative curve indicating the spatial resolution. The spatial resolution is evaluated to be 71.4 μm that is the similar to the diffraction limit.

References

[1] S. Kimura et al., Nucl. Instrum. Meth. A **467-468**, 893 (2001).

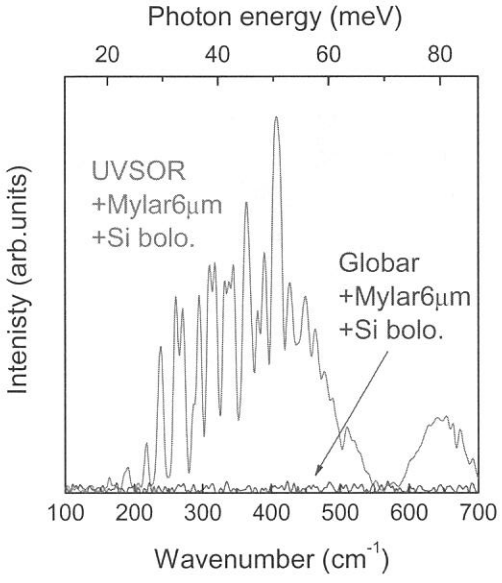

Fig. 1. Throughput spectra of IR microscope at BL6A1 using UVSOR and a globar lamp.

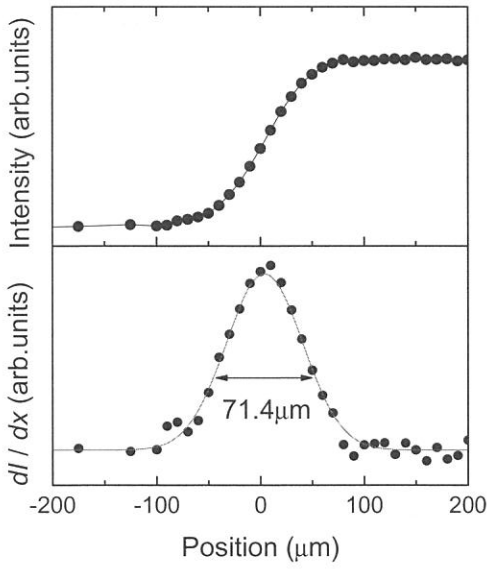

Fig. 2. (a) Intensity plot at an edge of a gold mirror vs scanning position. (b) First derivative curve of figure (a). This means the spatial resolution of the microscope in the wavenumber region of Fig. 1.

Design of new infrared and terahertz beamline BL6B at UVSOR

S. Kimura[1,2], E. Nakamura[1], J. Yamazaki[1], M. Katoh[1], T. Nishi[2], H. Okamura[3], M. Matsunami[3], L. Chen[3] and T. Nanba[3]

[1]*UVSOR Facility, Institute for Molecular Science, Okazaki 444-8585*
[2]*Department of Structural Molecular Science, The Graduate School for Advanced Studies, Okazaki 444-8585*
[3]*Graduate School of Science and Technology, Kobe University, Kobe 657-8501*

We have designed a new infrared beamline, BL6B, for infrared and terahertz spectroscopies including microspectroscopy with high brilliance and high flux. The beamline will be replaced in the spring of 2004 from the infrared beamline, BL6A1, at UVSOR that was firstly opened for users in 1985. [1] The beamline made an important contribution to the development of IR-SR science. In 2002-2003, UVSOR is upgraded to a high brilliance light source. [2] Due to the upgrading, the infrared beamline is also replaced to a new one with a large acceptance angle. The main purpose of the beamline is spectromicroscopy for development of new materials in the infrared and terahertz regions. Here, the beamline design and the expected performance are reported.

The design concepts are the followings.

(1) Higher photon flux and higher brilliance than old beamline, BL6A1.
(2) The place of the end station does not shift because of the keeping of the experimental area.

To achieve (1), a collecting mirror is set in a bending magnet chamber as shown in Figure 1. The IR light is led to the focal point by three mirrors, first is the collecting mirror, the others plane mirrors. The acceptance angle becomes 215(H) × 80(V) mrad^2 that is about four times larger than BL6A1 (80(H) × 60(V) mrad^2). For the focusing of the light with the large acceptance angle, we employed a perfect focusing mirror to the circular trajectory, so-called "magic mirror" that has been successfully installed at the IR beamline of SPring-8. [3] To avoid the heat load from the synchrotron radiation to the mirror, a part on the orbital plane is covered by a copper plate with water cooling. The expected beam size at the focal point by a ray trace method is shown in Figure 2. The beam size at $h\nu$ = 0.1 eV was calculated to be 2(H) × 1(V) mm^2 that is much smaller than that of BL6A1 (about 5(H) × 3(V) mm^2).

The calculated photon flux and brilliance are shown in Figures 3 and 4. The photon flux of BL6B is about four times higher than that of the BL6A1 and one order larger than that of the IR beamline, BL43IR, at SPring-8 because of the large acceptance angle.

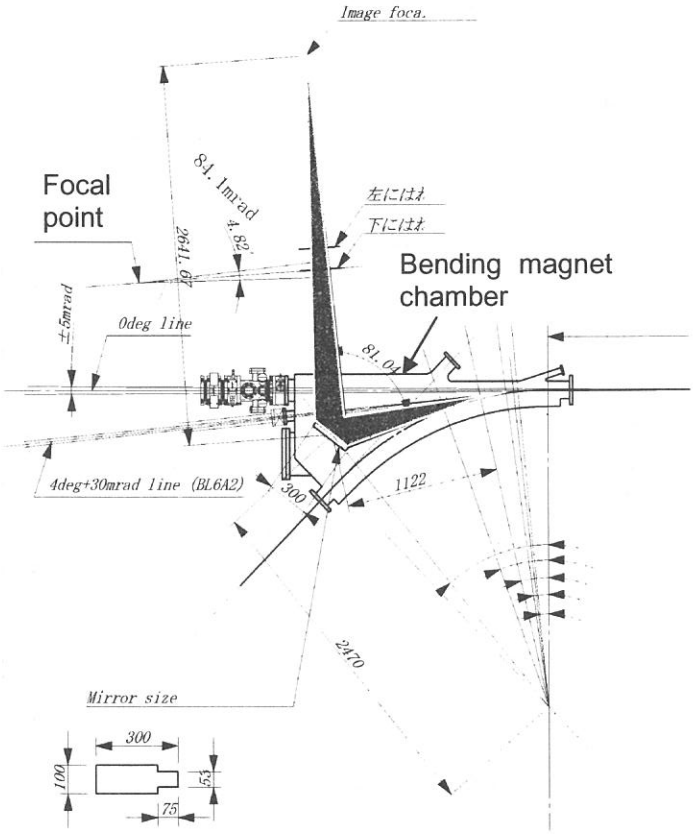

Fig. 1. Optics layout of the new infrared and terahertz beamline, BL6B. The first focusing mirror that is a "magic mirror" is located in the bending magnet chamber.

On the other hand, the brilliance becomes one order higher than that of BL6A1 as shown in Fig. 4 because of the smaller focal size. However, the brilliance above $h\nu$ = 0.1 eV is still one order lower than that of SPring-8 BL43IR because the bending radius of SPring-8 is about one order larger than that of UVSOR. However, considering a diffraction effect, the brilliance of BL6B is higher than that of SPring-8 BL43IR in the terahertz region below $h\nu$ = 0.01 eV. Therefore experiments using the high brilliance in the terahertz region, for instance terahertz microspectroscopy, are suitable for the beamline.

References

[1] T. Nanba *et al.*, Int. J. Infrared and Millimeter Waves **7**, 1769 (1986).
[2] M. Katoh *et al.*, Nucl. Instrum. Meth. A **467-468**, 68 (2001).
[3] S. Kimura *et al.*, Nucl. Instrum. Meth. A **467-468**, 437 (2001).

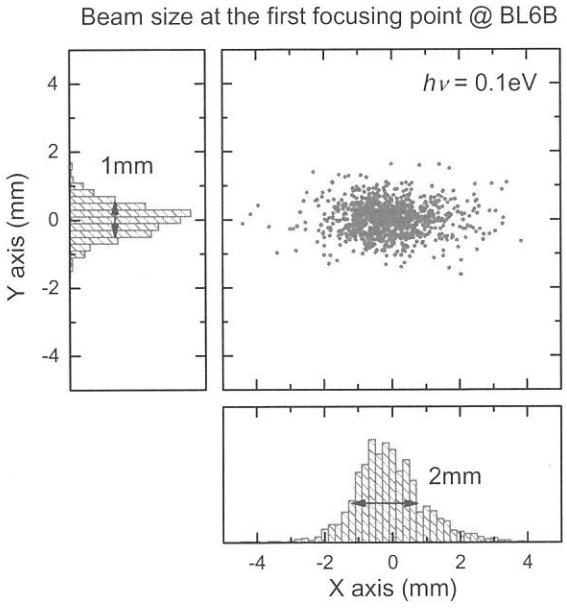

Fig. 2. Ray trace result at the focal point at the photon energy of $h\nu$ = 0.1 eV.

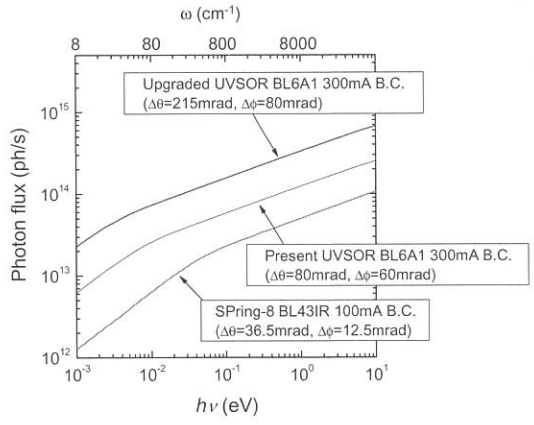

Fig. 3. Calculated photon flux spectra of BL6B and BL6A1 of UVSOR and BL43IR of SPring-8.

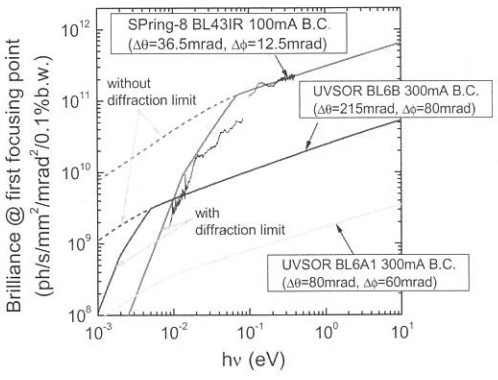

Fig. 4. Calculated brilliance spectra of BL6B and BL6A1 of UVSOR and BL43IR of SPring-8 with diffraction effect. Measured brilliance spectrum at BL43IR is also plotted.

(BL8A)

Carbon contamination of SR mirror

Mikito Tadano[1], Takashi Naito[1], Eiken Nakamura[2], Masami Hasumoto[2],
Hiroshi Sakai[3], Takashi Shibuya[3], Eiji Shigemasa[2], Junji Urakawa[1]

[1] *High Energy Accelerator Research Organization, 1-1 Oho Tsukuba 305-0801,Japan*
[2] *Institute for Molecular Science, Okazaki 444-8585,Japan*
[3] *The institute for solid statephysics*

A carbon contamination of an optical device is a serious problem for the SR experiment and measurement. The carbon contamination reduces the reflectivity of the optical device and deteriorates the measurement performance.

In the current fiscal years, we investigated the carbon contamination by using glass mirrors with several conditions. The thermal condition of the glass mirror was not good when irradiate the SR for the thermal conductivity. The measured reflectivity was included the thermal damage. So we used temperature controlled cupper mirrors in this experiment. Fig1 shows the change of the reflectance of the cupper mirror when irradiate SR with several conditions. The clear difference was observe when apply an oil to the mirror surface directly. The reflectivity is reduced to less than 20% when after 6 hours irradiate the SR. 5% reflectivity reduction was observed in the case of the oil included in vacuum condition. In the cases of the include CO_2, CH_4, and the different mirror temperature condition of 10 degreeC, 25 degreeC, 50 degreeC showed same reflectivity reduction 2~3%.

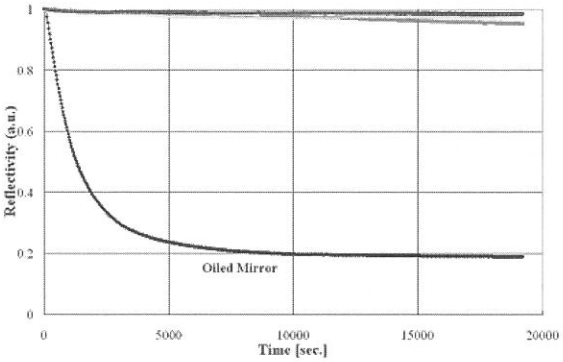

fig.1:Reflectivity of irradiated mirror
The lowest line: Oiled mirror
The other upper lines: CO2,CH4, 10degeeC, 25degeeC,50degreeC, and Oiled flange.

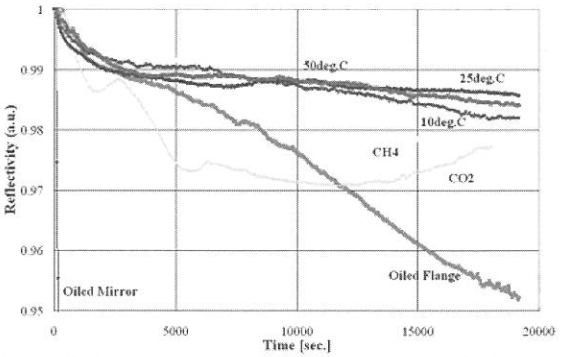

fig.2: The upper part of fig.1.is expanded. They are 25degeeC, 50degeeC, 10degeeC, CH_4 gas, CO_2 gas, and Oiled flange from a top line.

Reference

[1] E.Nakamura et.al., UVSOR Activity Report,2001,P49
[2] T.Naito et.al., UVSOR Activity Report, 2000,P63